

Published in final edited form as:

*Circ Res.* 2008 June 20; 102(12): 1492–1501. doi:10.1161/CIRCRESAHA.107.168070.

## Deficiency of Adipose Differentiation-Related Protein Impairs Foam Cell Formation and Protects Against Atherosclerosis

Antoni Paul<sup>1</sup>, Benny Hung-Junn Chang<sup>2</sup>, Lan Li<sup>2</sup>, Vijay K. Yechoor<sup>1</sup>, and Lawrence Chan<sup>1,2,\*</sup>

<sup>1</sup>Department of Medicine, Baylor College of Medicine, One Baylor Plaza, Houston, Texas 77030

<sup>2</sup>Department of Molecular & Cellular Biology, Baylor College of Medicine, One Baylor Plaza, Houston, Texas 77030

### Abstract

Foam cells are a hallmark of atherosclerosis. However, it is unclear if foam cell formation *per se* protects against atherosclerosis or fuels it. In this study we investigated the role of adipose differentiation-related protein (ADFP), a major lipid-droplet protein (LDP), in the regulation of foam cell formation and atherosclerosis. We show that ADFP expression facilitates foam cell formation induced by modified lipoproteins in mouse macrophages *in vitro*. We show further that *Adfp* gene inactivation in apolipoprotein E-deficient (*ApoE*<sup>-/-</sup>) mice reduces the number of lipid droplets in foam cells in atherosclerotic lesions and protects the mice against atherosclerosis. Moreover, transplantation of ADFP-null bone marrow-derived cells effectively attenuated atherosclerosis in *ApoE*<sup>-/-</sup> mice. Deficiency of ADFP did not cause a detectable compensatory increase in the other PAT-domain proteins in macrophages *in vitro* or *in vivo*. Mechanistically, ADFP enables the macrophage to maintain its lipid content by hindering lipid efflux. We detected no significant difference in lesion composition or in multiple parameters of inflammation in macrophages or in their phagocytic activity between mice with and without ADFP. In conclusion, *Adfp* inactivation in *ApoE*<sup>-/-</sup> background protects against atherosclerosis and appears to be a relatively pure model of impaired foam cell formation.

### Keywords

ADFP; atherosclerosis; foam cells; lipid droplets

The lipid-laden macrophage or “foam cell” is a hallmark of atherosclerosis<sup>1,2</sup>. Foam cell formation is generally thought of as a protective mechanism whereby the vessel wall rids itself of potentially harmful lipids. Furthermore, macrophages, whether engorged with lipids or not, play a key role in the mediation and modulation of inflammation, and much atherosclerosis research has targeted the role of macrophages in the inflammation pathways that underlie atherogenesis<sup>3,4</sup>. Nonetheless, atherosclerosis is more than inflammation of the artery (or arteritis,<sup>5,6</sup>); despite some overlap in pathology, there are differences between atherosclerotic and non-atherosclerotic arteritis<sup>7</sup>. A fundamental question in the field remains: how crucial is unfettered lipid accumulation in macrophages in protecting against or fueling atherosclerosis progression, or, alternatively, whether an inherent impairment in the macrophages’ ability to accumulate lipid in an animal alters its susceptibility to atherosclerosis.

Correspondence should be addressed to L.C. (lchan@bcm.edu).

**Disclosures:** none.

Lipids do not occur free in the cytoplasm of foam cells, but are sequestered inside special “bags” called lipid droplets (LDs) or fat bodies. These structures are stabilized and circumscribed by lipid droplet proteins (LDPs)<sup>8,9</sup>. A large number of proteins are associated with LDs, and the most abundant and unique LDPs that occur in lipid-laden cells of the body are the PAT-domain proteins, named after perilipin (PLIN)<sup>10,11</sup>, adipose differentiation-related protein (ADFP), and tail-interacting protein of 47 kDa (TIP47)<sup>12,13</sup>. More recently, another LDP, S3-12<sup>14</sup>, has been classified in the same group<sup>8,9</sup>. It is reasonable to hypothesize that the PAT-domain proteins play an enabling role in lipid accumulation in macrophages.

In this communication, we show that ADFP plays a key role in foam cell formation, and its absence severely restricts the macrophages' ability to become foam cells *in vitro*. Furthermore, we found that ADFP is the most upregulated PAT-domain protein in atheromas. We then used the atherosclerosis-prone *ApoE*<sup>-/-</sup> mice to show that genetic ablation of ADFP expression greatly restricts foam cell formation *in vivo*, and this “defect” alone is sufficient to protect these mice against atherosclerosis development. The study demonstrates that foam cell formation *per se*, without perturbation in the inflammatory balance, is a crucial pathogenic event in atherosclerosis development.

## Methods

### Mice

*Adfp*<sup>-/-</sup> mice in C57BL/6J background (F8)<sup>15</sup> were crossed two times with *ApoE*<sup>-/-</sup> mice (B6.129P2-Apoe<sup>tm1Unc</sup>, Jackson Laboratories) to generate *ApoE*<sup>-/-</sup>/*Adfp*<sup>+/-</sup> mice. These mice were used as breeding pairs to generate the *ApoE*<sup>-/-</sup>/*Adfp*<sup>-/-</sup> and *ApoE*<sup>-/-</sup>/*Adfp*<sup>+/+</sup> littermates used in the study. Atherosclerosis development was analyzed in male and female mice of both genotypes at 20 weeks of age. For the bone marrow (BM) transfer study, 22 8-week old *ApoE*<sup>-/-</sup> females were distributed into two groups with similar CHOL levels, subjected to 10 Gy total body irradiation, and the BM reconstituted with cells from *ApoE*<sup>-/-</sup>/*Adfp*<sup>-/-</sup> or *ApoE*<sup>-/-</sup>/*Adfp*<sup>+/+</sup> mice. Atherosclerosis development was analyzed 14 weeks after BM transfer. Plasma CHOL and TG levels were measured using kits from Thermo Electron. Plasma lipoproteins were fractionated by fast-performance liquid chromatography gel filtration using Superose 6B columns (Pharmacia LKB Biotechnology). Mice had free access to regular chow and water along the study. All animal experiments were conducted following protocols approved by the Institutional Animal Care and Use Committee at Baylor College of Medicine.

### Analysis of atherosclerotic lesions

We measured atherosclerosis development in six sections of the aortic sinus spanning the region from the very proximal aorta to the point that contains three complete leaflets based on the method of Paigen *et al.*<sup>16</sup> as previously described<sup>17,18</sup>. We performed immunohistochemistry using primary antibodies specific for ADFP (Progen), PLIN (Progen), TIP47 (a gift from Dr. C. Sztalryd, University of Maryland, Baltimore, MD), S3-12 (a gift from Dr. PE Bickel, University of Texas, Houston, TX), and Macrophages (Mac-3, Santa Cruz Biotechnology), as previously described<sup>18</sup>. TUNEL staining was performed using kits from Promega. Stainings with Hematoxylin & Eosin, Masson's trichrome, Pearls' (iron) and Van Kossa (calcium) were performed using standard protocols.

### Electron microscopy (EM) analysis of atherosclerotic lesions

Aortic sinuses were processed in the Integrated Microscopy Core at Baylor College of Medicine. Images of foam cells in random sections of three pairs of *Adfp*<sup>+/+</sup>/*ApoE*<sup>-/-</sup> and *Adfp*<sup>-/-</sup>/*ApoE*<sup>-/-</sup> littermates were taken at 4000× with a Hitachi H-7500 microscope. The

total area of the sections, the number and the area of the LDs were analyzed in triplicate using the AxioVision image-analysis system (Carl Zeiss Vision).

### Experiments in cultured macrophages

RAW 264.7 macrophages were cultured following standard procedures. Thioglycollate-elicited peritoneal macrophages were harvested as previously described<sup>19</sup>. In some experiments 50 µg/ml of acLDL or oxLDL (Intracel Resources) were added to the culture media. To visualize LDs, oil red O and Nile red stainings were performed following standard procedures. Binding and uptake of DiI-acLDL were analyzed as previously described<sup>20</sup>. For [<sup>3</sup>H]cholesterol labeling, the cells were incubated in DMEM 0.2% BSA containing acLDL (50 µg/ml) labeled with [<sup>3</sup>H]cholesterol (Amersham; specific activity 142470 cpm/µg acLDL). To study the efflux of [<sup>3</sup>H]cholesterol, after labeling, washing and equilibrating, the cells were incubated with DMEM 0.2% BSA containing human apoA-I (10 µg/ml; Intracel Resources). Aliquots of the media were collected at different timepoints and immediately centrifuged to remove cell debris. At the final timepoint, the cells were lysed and the radioactivity in the cells and in the supernatants were determined by scintillation counting. To estimate the rate of intracellular cholesterol ester (CE) accumulation, peritoneal macrophages were exposed to 50 µg/ml of cold acLDL for 20 hours, washed and pulsed with [9,10 (n) <sup>3</sup>H]oleic acid complexed with BSA (molar ratio oleic acid to BSA 1:3; specific activity of oleic acid 7034 cpm/nmol) for 4 and 24 hours. Lipid fractions were separated by thin-layer chromatography (TLC) and the amount of [9,10 (n) <sup>3</sup>H] oleic acid incorporated into CEs determined by scintillation counting. Microsomal acyl-coA:cholesterol acyltransferase (ACAT) activity was determined by measuring the rate of incorporation of [<sup>14</sup>C]oleoyl-CoA into the CE fraction as previously described<sup>21</sup>. To determine CE hydrolase activity, cells were loaded with cold acLDL (50 µg/ml, O/N), washed and pulsed with [9,10 (n) <sup>3</sup>H] oleic acid for 24 hours. Cholesterol esterification was blocked with the ACAT inhibitor CP113818 (10 µM, a gift from Dr. TY Chang, Dartmouth Medical School, Hanover, NH), apoA-I (10µg/ml) was added to the culture media and the rate of disappearance of intracellular <sup>3</sup>H-labeled CE was analyzed by TLC at 3, 6, 9 and 23 h.

Cellular lipids were extracted with hexane:isopropanol (3v:2v) and protein pellets were dissolved in 0.2 N NaOH, neutralized with HCl and measured with enzymatic kits (Bio-Rad Laboratories). For TLC, the total lipids were evaporated to dryness, re-dissolved in chloroform, spotted on silica gel plates, and separated using hexane-diethyl ether-glacial acetic acid (75:35:1) as previously described<sup>15</sup>.

### Western-blot and Real-Time quantitative PCR (qPCR) analysis

Western blotting and qPCRs were performed as described<sup>18,19</sup>. Primer sequences are available in supplemental data online. Relative gene expression levels were determined from threshold cycle (Ct) values normalized to GAPDH.

### Statistical Analysis

Data were analyzed using SPSS 11.0 for Windows. Statistical analyses were carried out using Mann-Whitney U or *t*-tests. Differences were considered significant when *p*<0.05. In all tables and figures, the results are expressed as mean ±SD.

## Results

### ADFP is the Major LDP Stimulated by Lipid Accumulation in Macrophages *in vitro* and in Atherosclerotic Lesions of ApoE<sup>-/-</sup> Mice

To tease out the proteins that empower macrophages to transform into foam cells, we first examined the mRNA level of different PAT-domain proteins in RAW 264.7 cells, a mouse macrophage cell line, cultured in the absence or presence of acetylated LDL (acLDL; 50 μg/ml for 24 hours). Under basal conditions, we could readily detect *Adfp* and *Tip47* transcripts. The addition of acLDL stimulated *Adfp* mRNA to ~180% of basal, but had no effect on the level of *Tip47* mRNA (Figure 1a and 1b). The basal level of *Plin* mRNA was barely detectable and substantially lower than that of *Adfp* and *Tip47*, and remained unchanged when acLDL was added (Figure 1a and 1b). We could not detect any *S3-12* mRNA whether or not acLDL was included in the incubation medium (Figure 1a and 1b). By immunoblot analysis (Figure 1c), ADFP and TIP47 were readily detectable in RAW264.7 cellular extracts. acLDL treatment significantly increased the intensity of the ADFP band (to ~180%) but was without effect on the intensity of the TIP47 band (Figure 1d). We were unable to detect immunoreactive PLIN or S3-12 either in the absence or presence of acLDL, indicating that the low level *Plin* mRNA present was not translated into a detectable amount of protein.

Next, we screened for the expression of mRNA for these proteins in atherosclerotic arteries in *C57BL/6 ApoE<sup>-/-</sup>* mice, comparing their levels to those of non-atherosclerotic *C57BL/6 ApoE<sup>+/+</sup>* mice. We harvested the aortas at 24 weeks of age, when the aortic sinuses of *ApoE<sup>-/-</sup>* mice were studded with atherosclerotic lesions, while those of wild-type *ApoE<sup>+/+</sup>* mice were free of atherosclerotic involvement. In contrast to the transcripts for *Plin*, *Tip47*, and *S3-12*, which showed no difference between *ApoE<sup>-/-</sup>* and wild-type mice, the level of *Adfp* mRNA increased to ~350% in the aortic sinuses of *ApoE<sup>-/-</sup>* mice (Figure 1e). Therefore, among the major LDPs, only the accumulation of ADFP correlates with lipid droplet accumulation in macrophages *in vitro*, and only *Adfp* expression is stimulated in the aortic sinuses *in vivo* in mice. These findings agree with previous reports showing that ADFP is highly upregulated in human atherosclerotic lesions<sup>22–24</sup>. We note that previous reports did not simultaneously examine all the major LDPs as we did.

### Absence of ADFP Restricts Atherosclerosis Development in ApoE<sup>-/-</sup> Mice

We next examined whether the absence of ADFP would affect atherosclerosis development in male and female *ApoE<sup>-/-</sup>/Adfp<sup>-/-</sup>* and *ApoE<sup>-/-</sup>/Adfp<sup>+/+</sup>* littermates. There was no difference in body weight, plasma CHOL and TG levels throughout the study (Online Table I). The mice also displayed identical plasma lipoprotein profiles whether or not they produced ADFP (Online Figures Ia and Ib). We sacrificed the mice at 20 weeks of age and compared the atherosclerotic lesion size in the aortic sinus areas (Figure 2a–2d). As previously observed in *ApoE<sup>-/-</sup>* mice, female animals developed larger lesions than males in both genotypes. In males, the lack of ADFP was associated with a 58% reduction in lesion size (from  $137 \pm 98 \times 10^3 \mu\text{m}^2$  to  $57 \pm 40 \times 10^3 \mu\text{m}^2$ ). In females there was similarly a significant reduction of 40% in lesion size in mice lacking ADFP (from  $575 \pm 213 \times 10^3 \mu\text{m}^2$  to  $345 \pm 153 \times 10^3 \mu\text{m}^2$ ). Therefore, the absence of ADFP protects against atherosclerosis development in both male and female *ApoE<sup>-/-</sup>* mice.

ADFP protein and mRNA are present in diverse cell types when they accumulate lipid<sup>25,26</sup>. In support of an important role for ADFP in fat accumulation is the fact that absence of ADFP decreases lipid accumulation in the liver when mice are fed a high-fat diet<sup>15</sup>. To exclude the possibility that absence of ADFP in other tissues accounts for the protection against atherosclerosis, we transferred BM cells from *ApoE<sup>-/-</sup>/Adfp<sup>-/-</sup>* or *ApoE<sup>-/-</sup>/Adfp<sup>+/+</sup>*

female mice to 8-week old *ApoE*<sup>-/-</sup>/*Adfp*<sup>+/+</sup> recipient female mice, and compared the extent of aortic atherosclerosis in the recipients 14 weeks after bone marrow transfer (Figure 2e). We found that mice that received BM from ADFP-deficient donors had smaller lesions compared with those that received bone marrow cells from *ApoE*<sup>-/-</sup>/*Adfp*<sup>+/+</sup> donors (size reduced from  $425 \pm 69 \times 10^3 \mu\text{m}^2$  *ApoE*<sup>-/-</sup>/*Adfp*<sup>+/+</sup> to  $322 \pm 71 \times 10^3 \mu\text{m}^2$ ). Therefore, absence of *Adfp* in bone marrow-derived cells alone is sufficient to protect against atherosclerosis in *ApoE*<sup>-/-</sup> mice.

### No Compensatory Upregulation of other major PAT-domain Proteins in the Absence of ADFP

To examine if other PAT domain proteins undergo compensatory upregulation when ADFP is missing, we isolated peritoneal macrophages from *ApoE*<sup>-/-</sup>/*Adfp*<sup>-/-</sup> and *ApoE*<sup>-/-</sup>/*Adfp*<sup>+/+</sup> mice, cultured them in the absence or presence of oxLDL, and quantified the mRNA for the different PAT-domain proteins by qPCR. As expected, *Adfp* mRNA was undetectable in the peritoneal macrophages of *ApoE*<sup>-/-</sup>/*Adfp*<sup>-/-</sup> mice but readily detectable in the *ApoE*<sup>-/-</sup>/*Adfp*<sup>+/+</sup> mice. Furthermore, *Adfp* mRNA concentration was significantly stimulated by exposure of *ApoE*<sup>-/-</sup>/*Adfp*<sup>+/+</sup> macrophages to oxLDL (Figure 3a and 3b). We could detect S3-12 and TIP47 mRNA, but not PLIN mRNA. However, we found no difference in any of these transcripts between cells with and without ADFP expression whether or not the macrophages were exposed to oxLDL, and exposure to oxLDL did not increase the expression of any of these genes (Figure 3a and 3b). Therefore, *Adfp*<sup>-/-</sup> macrophages did not overexpress TIP47 as was observed in fibroblastic cell lines isolated from *Adfp*<sup>-/-</sup> embryos<sup>27</sup>; they were much more like *Adfp*<sup>-/-</sup> liver cells<sup>15</sup>, which also did not upregulate the production of TIP47 or other PAT-domain proteins.

As PAT-domain proteins have been shown to exhibit substantial post-translational regulation<sup>28</sup>, we next analyzed protein expression by immunoblotting (Figure 3c). We found TIP47, but not PLIN or S3-12, in extracts of macrophages isolated from *ApoE*<sup>-/-</sup>/*Adfp*<sup>-/-</sup> and *ApoE*<sup>-/-</sup>/*Adfp*<sup>+/+</sup> mice. As expected, ADFP was detected only in *ApoE*<sup>-/-</sup>/*Adfp*<sup>+/+</sup> animals. The relative concentration of immunoreactive TIP47 was the same whether or not the macrophages expressed ADFP. Furthermore, in contrast to ADFP, the expression of TIP47 protein was not affected by the addition of oxLDL. This oxLDL-regulated *Adfp* expression and absence of an effect on *Tip47* expression is consistent with that observed in acLDL-regulated gene expression in RAW 264.7 cells (Figure 1). To determine if the lack of compensation of TIP47 extends to the *in vivo* situation, we quantified the amount of *Tip47* mRNA in the RNA isolated from the aortic sinus of *ApoE*<sup>-/-</sup> mice and found that the concentration of *Tip47* mRNA did not differ between mice that expressed ADFP and those that did not (Figure 3d). Next, we analyzed sections of aortic sinus lesions of *ApoE*<sup>-/-</sup>/*Adfp*<sup>-/-</sup> and *ApoE*<sup>-/-</sup>/*Adfp*<sup>+/+</sup> mice by immunohistochemistry. We readily detected ADFP and TIP47 (Figure 3e and 3f), but not PLIN or S3-12 in the lesions (Figure 3g and 3h). In addition, the relative distribution and density of immunoreactive TIP47 in the aortic sinus lesions was similar in *ApoE*<sup>-/-</sup>/*Adfp*<sup>-/-</sup> vs. *ApoE*<sup>-/-</sup>/*Adfp*<sup>+/+</sup> mice (Figure 3i).

### Absence of ADFP Restricts Foam Cell Formation

The rationale for the experiments on atherosclerosis development in the two types of *ApoE*<sup>-/-</sup> mice is based on the hypothesis that ADFP modulates foam cell formation in these animals. To assess whether this is true, we first used peritoneal macrophages isolated from *ApoE*<sup>-/-</sup>/*Adfp*<sup>-/-</sup> and *ApoE*<sup>-/-</sup>/*Adfp*<sup>+/+</sup> mice as an *in vitro* model. As shown in Figure 4a–4c, the lack of ADFP reduced significantly the accumulation of LDs after overnight incubation with oxLDL. Similar experiments performed in macrophages isolated from *C57BL/6/ApoE*<sup>+/+</sup> mice yielded comparable results (Online Figure II). Next, we examined the aortic sinus lesions by transmission EM. Atherosclerotic plaques from both *ApoE*<sup>-/-</sup>/*Adfp*<sup>-/-</sup>

*Adfp*<sup>+/+</sup> and *ApoE*<sup>-/-</sup>/*Adfp*<sup>-/-</sup> mice contained lipid-laden foam cells (Figure 4d and 4e). However, the number of LDs per unit area was reduced by >50% in lesions of mice lacking ADFP (Figure 4f). Interestingly, size distribution analysis revealed that the decrease in the number of intracellular LDs affected droplets of all sizes in lesions of *ApoE*<sup>-/-</sup>/*Adfp*<sup>-/-</sup> mice (Figure 4g). Thus, the effect of ADFP on foam cell formation *in vitro* is reflected in atherosclerotic lesions *in vivo*.

### Histopathological Analysis of Atherosclerotic Lesions and Atherosclerosis-related Macrophage Functions

As expected, small lesions, commonly observed especially in male mice, consisted mainly of fatty streaks with macrophage infiltration, whereas the larger lesions, found mainly in females, contained much more abundant collagen deposition and necrotic cores (Online Figure III). Quantitative analysis of lesions of female mice of both genotypes showed no significant differences in the density of apoptotic cells, total cell number content and macrophage content, collagen-positive or calcium-staining area or necrotic core areas (Online Figure IVa–IVg). Furthermore, the lack of ADFP did not affect the appearance of iron deposition, a marker of intraplaque hemorrhage, which was very scarce in mice of either genotype (Online Figure IVh).

Corroborating the findings *in vivo*, we observed a similar rate of apoptosis when peritoneal macrophages from *ApoE*<sup>-/-</sup>/*Adfp*<sup>+/+</sup> and *ApoE*<sup>-/-</sup>/*Adfp*<sup>-/-</sup> mice were cultured in the presence of acLDL (50 µg/ml) for 24 h (Online Figure V). We also found that the expression of cytokines (TNFα, IL1-α, IL1-β, CXCL1, CXCL2, IL-10, IL-6, JE and mCSF), cytokine receptors (CCR1, CCR2, CCR3 and CCR5) and iNOS, under basal conditions and after exposure to 50 µg/mL of oxLDL for 24 h, was similar in the two genotypes (Online Figure VI). Furthermore, the expression of these genes was also similar in aortic sinuses of *ApoE*<sup>-/-</sup>/*Adfp*<sup>+/+</sup> and *ApoE*<sup>-/-</sup>/*Adfp*<sup>-/-</sup> mice (Online Figure VII). Finally, we detected no difference in NO production and phagocytic activity in macrophages from mice with and without ADFP expression (Online Figure VIII and IX).

In sum, we found no difference in macrophage functions that have been associated with protection or propensity to develop atherosclerosis in mice that express or do not express ADFP. The only difference thus seems to be their capacity to accumulate lipid. We next examined how the lack of ADFP affects this property.

### Mechanism of Reduced Lipid Accumulation in Macrophages without ADFP

We used peritoneal macrophages to assess if the lack of ADFP affects CHOL trafficking. First, we used DiI-acLDL, a fluorescence-labeled acLDL, to assess if the absence of ADFP affects lipoprotein binding or uptake and found no differences in either process between macrophages isolated from *ApoE*<sup>-/-</sup>/*Adfp*<sup>-/-</sup> and *ApoE*<sup>-/-</sup>/*Adfp*<sup>+/+</sup> mice (Figure 5a). To more accurately quantify cholesterol uptake, we cultured peritoneal macrophages with [1α, 2α(N)-<sup>3</sup>H]cholesterol-labeled acLDL in the absence of extracellular acceptors and measured the intracellular [1α, 2α(N)-<sup>3</sup>H]cholesterol at 4 and 16 h by scintillation counting. Again, there was no difference between the two genotypes (Figure 5b). After lipoproteins are taken up by macrophages, CE are hydrolyzed in the endocytic compartment by the lysosomal acid lipase and free cholesterol (FC) is exported to other cellular sites, such as the plasma membrane, where it can remain as a structural component or be effluxed to extracellular acceptors, or the endoplasmic reticulum (ER), where it can be re-esterified by ACAT-1 and stored in cytoplasmic LDs<sup>29,30</sup>. We used [1α, 2α(N)-<sup>3</sup>H]CHOL-labeled macrophages to assess whether absence of ADFP influences cholesterol efflux to a plasma acceptor, apoA-I. As shown in Figure 5c, the amount of CHOL effluxed increased over time in both *ApoE*<sup>-/-</sup>/*Adfp*<sup>-/-</sup> and *ApoE*<sup>-/-</sup>/*Adfp*<sup>+/+</sup> cells; however, at the 16 h timepoint the CHOL effluxed was

57.5% higher in *ApoE*<sup>-/-</sup>/*Adfp*<sup>-/-</sup> cells ( $13.7 \pm 2.1\%$  vs.  $8.7 \pm 3.5\%$  in *ApoE*<sup>-/-</sup>/*Adfp*<sup>+/+</sup> cells, Figure 5c). Next, we measured the incorporation of [9,10 (n) <sup>3</sup>H] oleic acid to the CE pool to assess the accumulation of newly synthesized CE. In this case the macrophages isolated from *ApoE*<sup>-/-</sup>/*Adfp*<sup>+/+</sup> macrophages presented a significant (93%) increase in newly synthesized CE accumulation ( $504 \pm 185$  nmol/mg protein in *ApoE*<sup>-/-</sup>/*Adfp*<sup>+/+</sup> cells vs.  $261 \pm 119$  nmol/mg protein in *ApoE*<sup>-/-</sup>/*Adfp*<sup>-/-</sup> cells, Figure 5d). To determine whether the higher CE accumulation is the result of increased microsomal ACAT activity, we performed subcellular fractionation of macrophages and measured ACAT activity in the microsomal fraction. As shown in Figure 5e, the ACAT activity was similar in microsomes isolated from *ApoE*<sup>-/-</sup>/*Adfp*<sup>+/+</sup> and *ApoE*<sup>-/-</sup>/*Adfp*<sup>-/-</sup> cells, suggesting that the higher CE accumulation in macrophages from *ApoE*<sup>-/-</sup>/*Adfp*<sup>+/+</sup> mice is caused by the action of ADFP in facilitating CE storage in LDs or in preventing CE from hydrolysis. To differentiate between these two possibilities, we determined whether the absence of ADFP affects the rate of hydrolysis of the stored CE. We found no difference in the rate of CE hydrolysis between macrophages that express and those that do not express ADFP (Figure 5f), suggesting a main role of ADFP in facilitating CE storage in LDs.

Finally, we examined by qPCR the expression of other key molecules involved in intracellular CHOL homeostasis, including (i) the principal receptors involved in modified LDL uptake: SR-A1 and CD36; (ii) major molecules involved in reverse cholesterol transport: ATP binding cassette A1 (ABCA1), ATP binding cassette G1 (ABCG1) and scavenger receptor BI (SR-BI); and (iii) other key molecules involved in intracellular lipid metabolism, including Nieman-Pick Type C1 protein (NPC1), ACAT-1, fatty acid-binding protein aP2 and hormone sensitive lipase (HSL). As shown in Figure 5g (with primer sequences in Online Table II), there were no differences in the expression level of any of these molecules when we compared macrophages of the two genotypes. Therefore, the data suggest that ADFP directly facilitates lipid storage in LDs, and its absence results in a detour of intracellular cholesterol towards efflux pathways.

## Discussion

In this study, we have addressed whether the process of foam cell formation *per se* is a key determinant in atherosclerosis progression. We have selected ADFP because of previous studies suggesting its possible involvement in foam cell formation. ADFP expression increases following lipid loading (with oleic acid, oxLDL, or acLDL) of human monocytes<sup>31</sup> or macrophage/monocytic cell lines<sup>24,32,33</sup>. *Adfp* mRNA is detected in macrophage/lipid-rich areas of endarterectomy specimens<sup>22</sup>, and the level is 3.5 fold higher in atherosclerotic lesions than in healthy areas of the same artery<sup>24</sup>. *Adfp* gene transfer stimulates lipid accumulation in mouse fibroblasts<sup>34</sup> and in human macrophages incubated with acLDL<sup>24</sup>. Moreover, siRNA knock-down of *Adfp* expression in THP-1 macrophages reduces TG, and total and esterified CHOL in these cells<sup>24</sup>.

To determine if other PAT-domain proteins increase their expression to compensate for the absence of ADFP, we measured their expression level in macrophages and found no difference between mice with or without *Adfp* expression. This contrasts with a collaborative study between us and Drs. C. Sztalryd and C. Londos in which we screened the same PAT-domain proteins and found that clonal embryonic fibroblastic cells isolated from the same *Adfp*<sup>-/-</sup> mice display increased *Tip47* expression<sup>27</sup>. On the other hand, *Adfp*<sup>-/-</sup> macrophages behave like *Adfp*<sup>-/-</sup> liver cells<sup>15</sup> in that absence of ADFP does not change the level of expression of *Tip47* or other PAT-domain protein genes. This lack of compensation suggests that lipid accumulation in macrophages may be limited by the total PAT-domain protein concentration, which stays consistently below wild-type levels in *Adfp*<sup>-/-</sup> mice. We note that many other proteins, which are present in lower concentrations than the PAT-

domain proteins, have been isolated from LDs<sup>35</sup>, and we cannot exclude the possibility that some of them are upregulated when ADFP is missing. Nonetheless, the data indicate that the impaired ability of *Adfp*<sup>-/-</sup> macrophages to form LDs is clearly not restored to normal by compensatory overexpression of other LDPs, if indeed it has taken place.

Lipid-laden foam cells form because they take up excess lipids, mainly from CHOL-rich LDL, or they are too slow in letting go of their lipids, having to store the excess CHOL in LDs. Another possible way to inhibit foam cell formation is by inactivating ACAT-1, as CHOL must be esterified in the ER before it can be stored in LDs. However, ACAT inactivation or inhibition in macrophages appears to be toxic to the cell, possibly because of excess FC trafficking to the ER membranes<sup>36</sup>, giving rise to downstream effects, including increased synthesis of cytokines<sup>37</sup>, macrophage apoptosis and accelerated atherosclerosis with grossly necrotic lesions<sup>38</sup>. In contrast, after close examination of lesions and cultured macrophages, we did not find any evidence of toxicity in *Adfp*<sup>-/-</sup> cells. Interestingly, a recent report by Zhao *et al.* showed that the transgenic expression of a neutral CE hydrolase, an enzyme that hydrolyzes the CE stored in LDs, enhances CHOL efflux and reduces atherosclerosis in mice<sup>39</sup>. Taken together, these data suggest that the LD may be a direct drug target for anti-atherosclerosis therapy.

Our findings indicate that *Adfp*<sup>-/-</sup> mice appear to be a relatively pure model of inhibition of foam cell formation. Macrophages isolated from *ApoE*<sup>-/-</sup>/*Adfp*<sup>-/-</sup> mice exhibit an impaired ability to accumulate intracellular LDs, but they do not differ in other properties that are known to affect atherosclerosis susceptibility such as the ability to produce inflammatory cytokines or in their phagocytic activity<sup>40</sup>. For many years foam cells have been considered a hallmark of atherosclerosis. Herein we have presented direct evidence that a relative failure of foam cell formation *per se* protects against atherosclerosis development.

## Supplementary Material

Refer to Web version on PubMed Central for supplementary material.

## Acknowledgments

### Sources of Funding

This study was supported by a National Institutes of Health grant HL-51586 (to L.C.). A.P. was supported in part by a Scientist Development Grant from the American Heart Association, National Research Program, # 0535118N. B.H.-J.C. was supported in part by a Public Health Service grant P30-DK56338. L.C. was supported in part by the Betty Rutherford Chair from the St. Luke's Episcopal Hospital and Baylor College of Medicine.

## References

1. Poole JC, Florey HW. Changes in the endothelium of the aorta and the behavior of macrophages in experimental atheroma of rabbits. *J Pathol Bacteriol* 1958;75:245–251. [PubMed: 13576305]
2. Still WJ, Marriott PR. Comparative morphology of the early atherosclerotic lesion in man and cholesterol-atherosclerosis in the rabbit; An electron microscopic study. *J Atheroscler Res* 1964;4:373–386. [PubMed: 14225221]
3. Lusis AJ. Atherosclerosis. *Nature* 2000;407:233–241. [PubMed: 11001066]
4. Libby P. Inflammation in atherosclerosis. *Nature* 2002;420:868–874. [PubMed: 12490960]
5. Seko Y. Giant cell and Takayasu arteritis. *Curr Opin Rheumatol* 2007;19:39–43. [PubMed: 17143094]
6. Jennette JC, Falk RJ. Nosology of primary vasculitis. *Curr Opin Rheumatol* 2007;19:10–16. [PubMed: 17143090]



7. Frostegard J. Atherosclerosis in patients with autoimmune disorders. *Arterio Thromb Vasc Biol* 2005;25:1776–1785.
8. Londos C, Brasaemle DL, Schultz CJ, Segrest JP, Kimmel AR. Perilipins, ADRP, and other proteins that associate with intracellular neutral lipid droplets in animal cells. *Semin Cell Dev Biol* 1999;10:51–58. [PubMed: 10355028]
9. Londos C, Sztalryd C, Tansey JT, Kimmel AR. Role of PAT proteins in lipid metabolism. *Biochimie* 2005;87:45–49. [PubMed: 15733736]
10. Egan JJ, Greenberg AS, Chang MK, Londos C. Control of endogenous phosphorylation of the major cAMP-dependent protein kinase substrate in adipocytes by insulin and beta-adrenergic stimulation. *J Biol Chem* 1990;265:18769–18775. [PubMed: 2172232]
11. Greenberg AS, Egan JJ, Wek SA, Garty NB, Blanchette-Mackie EJ, Londos C. Perilipin, a major hormonally regulated adipocyte-specific phosphoprotein associated with the periphery of lipid storage droplets. *J Biol Chem* 1991;266:11341–11346. [PubMed: 2040638]
12. Diaz E, Pfeffer SR. TIP47: a cargo selection device for mannose 6-phosphate receptor trafficking. *Cell* 1998;93:433–443. [PubMed: 9590177]
13. Than NG, Sumegi B, Than GN, Bohn H. Cloning and sequence analysis of cDNAs encoding human placental tissue protein 17 (PP17) variants. *Eur J Biochem* 1998;258:752–757. [PubMed: 9874244]
14. Scherer PE, Bickel PE, Kotler M, Lodish HF. Cloning of cell-specific secreted and surface proteins by subtractive antibody screening. *Nat Biotechnol* 1998;16:581–586. [PubMed: 9624692]
15. Chang BHJ, Li L, Paul A, Taniguchi S, Nannegari V, Heird WC, Chan L. Protection against fatty liver but normal adipogenesis in mice lacking adipose differentiation-related protein. *Mol Cell Biol* 2006;26:1063–1076. [PubMed: 16428458]
16. Paigen B, Morrow PA, Holmes D, Mitchell D, Williams RA. Quantitative assessment of atherosclerotic lesions in mice. *Atherosclerosis* 1987;68:231–240. [PubMed: 3426656]
17. Calleja L, Paris MA, Paul A, Vilella E, Joven J, Jimenez A, Beltran G, Uceda M, Maeda N, Osada J. Low-cholesterol and high-fat diets reduce atherosclerotic lesion development in ApoE-knockout mice. *Arterioscler Thromb Vasc Biol* 1999;19:2368–2375. [PubMed: 10521366]
18. Paul A, Ko KWS, Li L, Yechoor V, McCrory MA, Szalai AJ, Chan L. C-reactive protein accelerates the progression of atherosclerosis in apolipoprotein E-deficient mice. *Circulation* 2004;109:647–655. [PubMed: 14744975]
19. Ko KW, Paul A, Ma K, Li L, Chan L. Endothelial lipase modulates HDL but has no effect on atherosclerosis development in apoE<sup>-/-</sup> and LDLR<sup>-/-</sup> mice. *J Lipid Res* 2005;46:2586–2594. [PubMed: 16199802]
20. Ricci R, Sumara G, Sumara I, Rozenberg I, Kurrer M, Akhmedov A, Hersberger M, Eriksson U, Eberli FR, Becher B, Boren J, Chen M, Cybulsky MI, Moore KJ, Freeman MW, Wagner EF, Matter CM, Luscher TF. Requirement of JNK2 for scavenger receptor A-mediated foam cell formation in atherogenesis. *Science* 2004;306:1558–1561. [PubMed: 15567863]
21. Becker A, Bottcher A, Lackner KJ, Fehringer P, Notka F, Aslanidis C, Schmitz G. Purification, cloning, and expression of a human enzyme with acyl-coenzyme-a -cholesterol acyltransferase activity, which is identical to liver carboxylesterase. *Arterioscler Thromb* 1994;14:1346–1355. [PubMed: 8049197]
22. Wang X, Reape TJ, Li X, Rayner K, Webb CL, Burnand KG, Lysko PG. Induced expression of adipophilin mRNA in human macrophages stimulated with oxidized low-density lipoprotein and in atherosclerotic lesions. *FEBS Lett* 1999;462:145–150. [PubMed: 10580108]
23. Forcheron F, Legedz L, Chinetti G, Feugier P, Letexier D, Bricca G, Beylot M. Genes of cholesterol metabolism in human atheroma - Overexpression of perilipin and genes promoting cholesterol storage and repression of ABCA1 expression. *Arterio Thromb Vasc Biol* 2005;25:1711–1717.
24. Larigauderie G, Furman C, Jaye M, Lasselin C, Copin C, Fruchart JC, Castro G, Rouis M. Adipophilin enhances lipid accumulation and prevents lipid efflux from THP-1 macrophages: potential role in atherogenesis. *Arterioscler Thromb Vasc Biol* 2004;24:504–510. [PubMed: 14707038]

25. Brasaemle DL, Barber T, Wolins NE, Serrero G, Blanchette-Mackie EJ, Londos C. Adipose differentiation-related protein is an ubiquitously expressed lipid storage droplet-associated protein. *J Lipid Res* 1997;38:2249–2263. [PubMed: 9392423]
26. Heid HW, Moll R, Schwetlick I, Rackwitz HR, Keenan TW. Adipophilin is a specific marker of lipid accumulation in diverse cell types and diseases. *Cell Tissue Res* 1998;294:309–321. [PubMed: 9799447]
27. Sztalryd C, Bell M, Lu XY, Mertz P, Hickenbottom S, Chang BHJ, Chan L, Kimmel AR, Londos C. Functional compensation for adipose differentiation-related protein (ADFP) by Tip47 in an ADFP null embryonic cell line. *J Biol Chem* 2006;281:34341–34348. [PubMed: 16968708]
28. Masuda Y, Itabe H, Odaki M, Hama K, Fujimoto Y, Mori M, Sasabe N, Aoki J, Arai H, Takano T. ADRP/adipophilin is degraded through the proteasome-dependent pathway during regression of lipid-storing cells. *J Lipid Res* 2006;47:87–98. [PubMed: 16230742]
29. Brown MS, Ho YK, Goldstein JL. The cholesteryl ester cycle in macrophage foam cells - Continual hydrolysis and re-esterification of cytoplasmic cholesteryl esters. *J Biol Chem* 1980;255:9344–9352. [PubMed: 7410428]
30. Maxfield FR, Wustner D. Intracellular cholesterol transport. *J Clin Invest* 2002;110:891–898. [PubMed: 12370264]
31. Buechler C, Ritter M, Duong CQ, Orso E, Kapinsky M, Schmitz G. Adipophilin is a sensitive marker for lipid loading in human blood monocytes. *Biochim Biophys Acta* 2001;1532:97–104. [PubMed: 11420178]
32. Chen JS, Greenberg AS, Tseng YZ, Wang SM. Possible involvement of protein kinase C in the induction of adipose differentiation-related protein by Sterol ester in RAW 264.7 macrophages. *J Cell Biochem* 2001;83:187–199. [PubMed: 11573236]
33. Robenek H, Lorkowski S, Schnoor M, Troyer D. Spatial integration of TIP47 and adipophilin in macrophage lipid bodies. *J Biol Chem* 2005;280:5789–5794. [PubMed: 15545278]
34. Imamura M, Inoguchi T, Ikuyama S, Taniguchi S, Kobayashi K, Nakashima N, Nawata H. ADRP stimulated lipid accumulation and lipid droplet formation in murine fibroblasts. *Am J Physiol Endocrinol Metab* 2002;283:E775–E783. [PubMed: 12217895]
35. Brasaemle DL, Dolios G, Shapiro L, Wang R. Proteomic Analysis of Proteins Associated with Lipid Droplets of Basal and Lipolytically Stimulated 3T3-L1 Adipocytes. *J Biol Chem* 2004;279:46835–46842. [PubMed: 15337753]
36. Feng B, Yao PM, Li YK, Devlin CM, Zhang DJ, Harding HP, Sweeney M, Rong JX, Kuriakose G, Fisher EA, Marks AR, Ron D, Tabas I. The endoplasmic reticulum is the site of cholesterol-induced cytotoxicity in macrophages. *Nat Cell Biol* 2003;5:781–792. [PubMed: 12907943]
37. Li YK, Tabas I. The inflammatory cytokine response of cholesterol-enriched macrophages is dampened by stimulated pinocytosis. *J Leukoc Biol* 2007;81:483–491. [PubMed: 17062603]
38. Fazio S, Major AS, Swift LL, Gleaves LA, Accad M, Linton MF, Farese RV. Increased atherosclerosis in LDL receptor-null mice lacking ACAT1 in macrophages. *J Clin Invest* 2001;107:163–171. [PubMed: 11160132]
39. Zhao B, Song J, Chow WN, St.Clair RW, Rudel LL, Ghosh S. Macrophage-specific transgenic expression of cholesteryl ester hydrolase significantly reduces atherosclerosis and lesion necrosis in *Ldlr*<sup>-/-</sup> mice. *J Clin Invest* 2007;117:2983–2992. [PubMed: 17885686]
40. Schrijvers DM, De Meyer GRY, Herman AG, Martinet W. Phagocytosis in atherosclerosis: Molecular mechanisms and implications for plaque progression and stability. *Cardiovas Res* 2007;73:470–480.

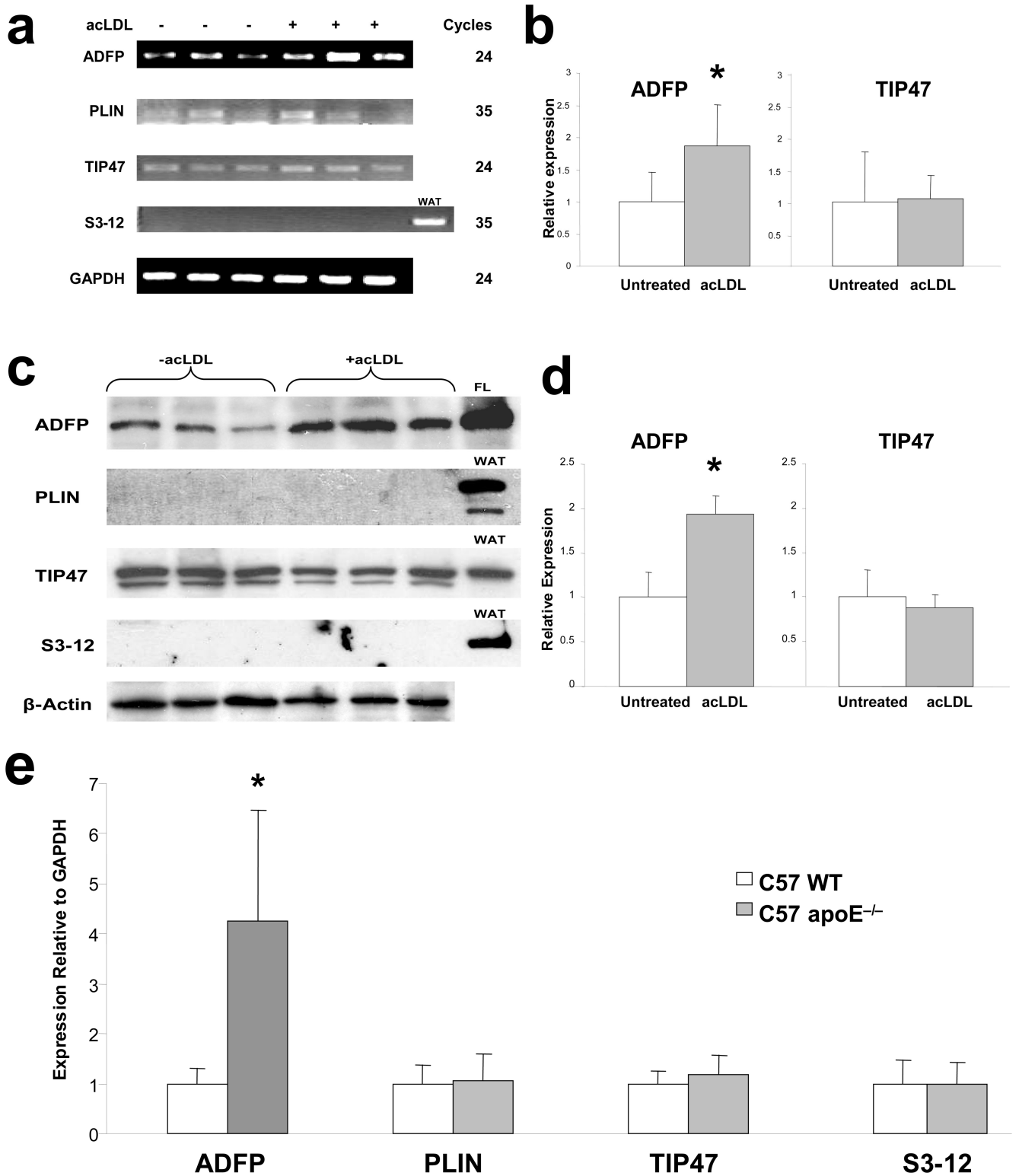
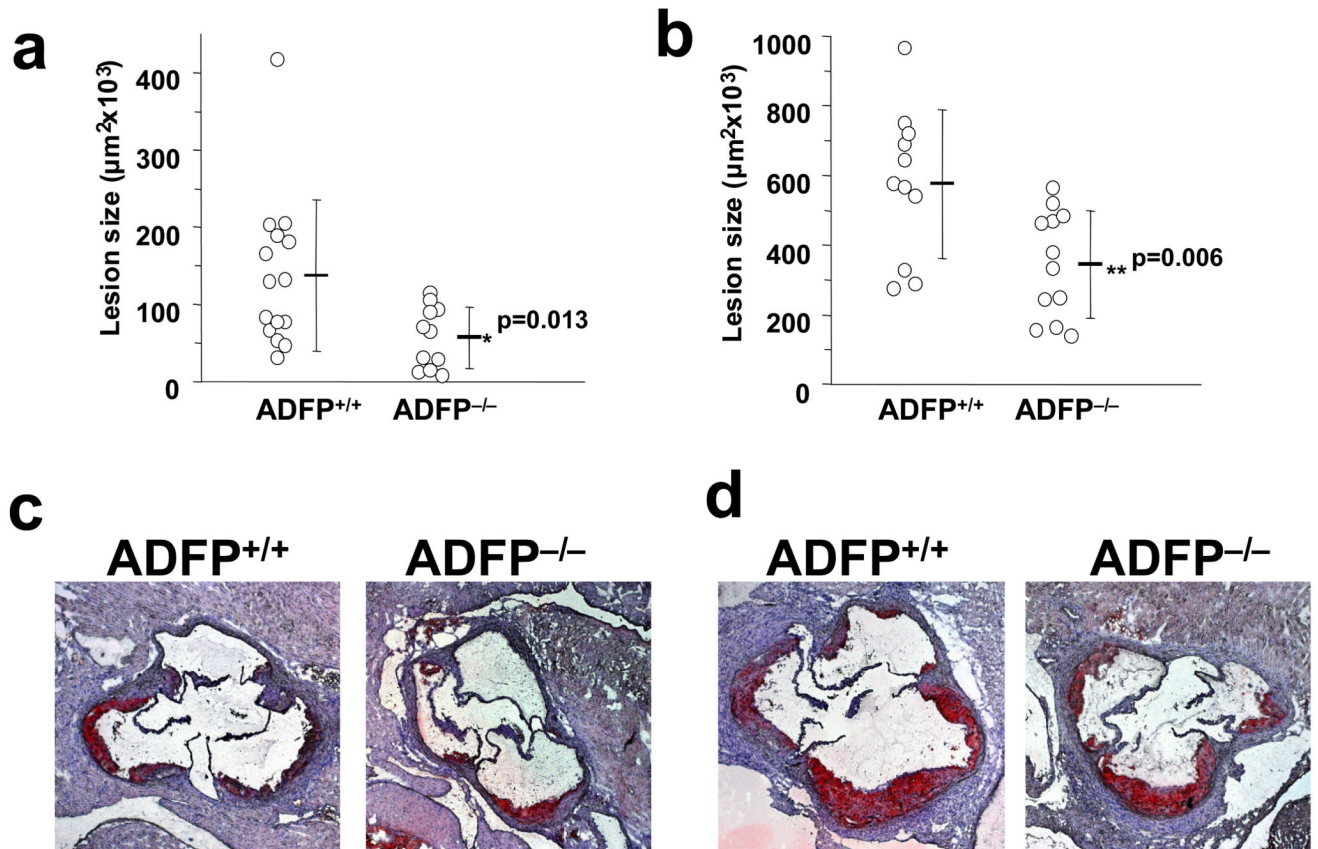
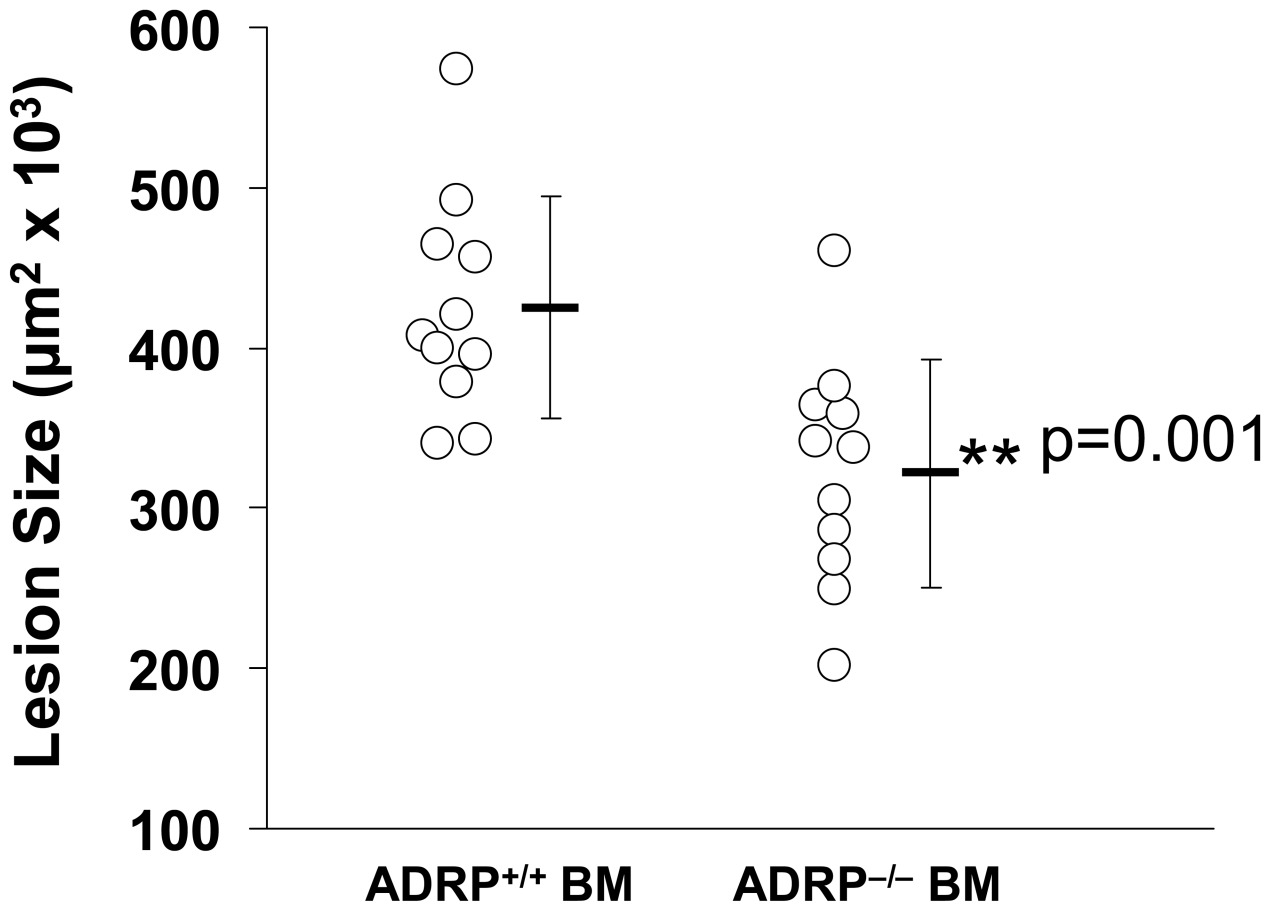


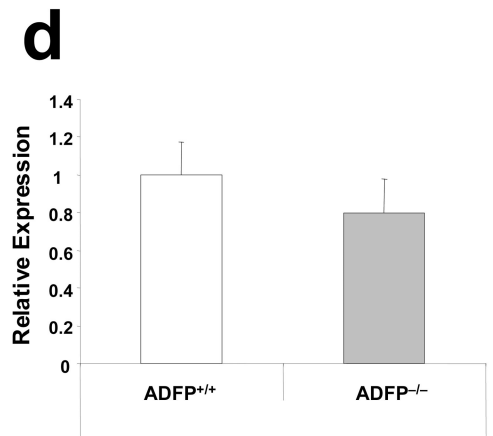
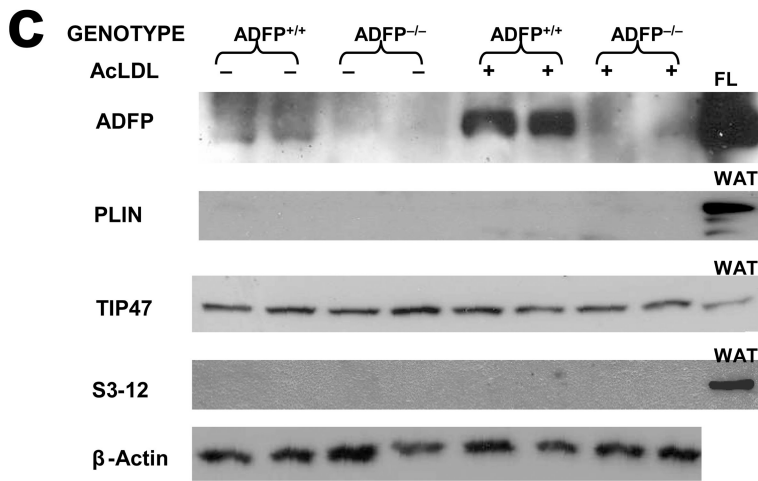
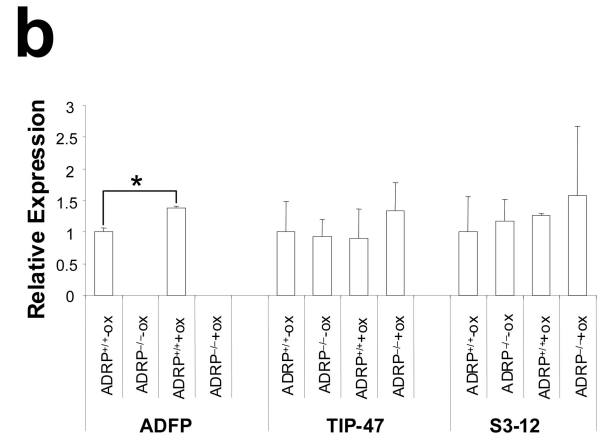
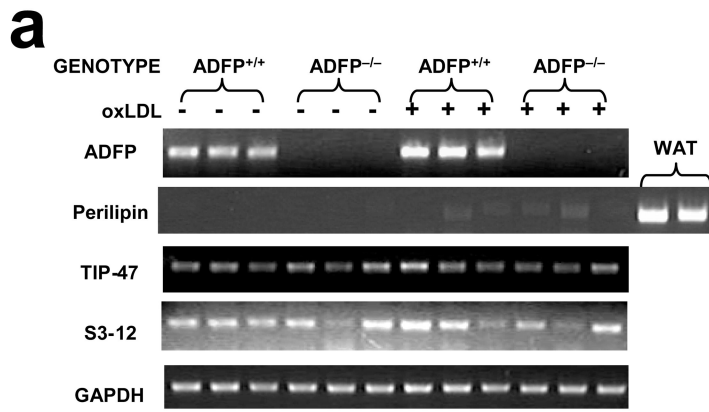
Figure 1.

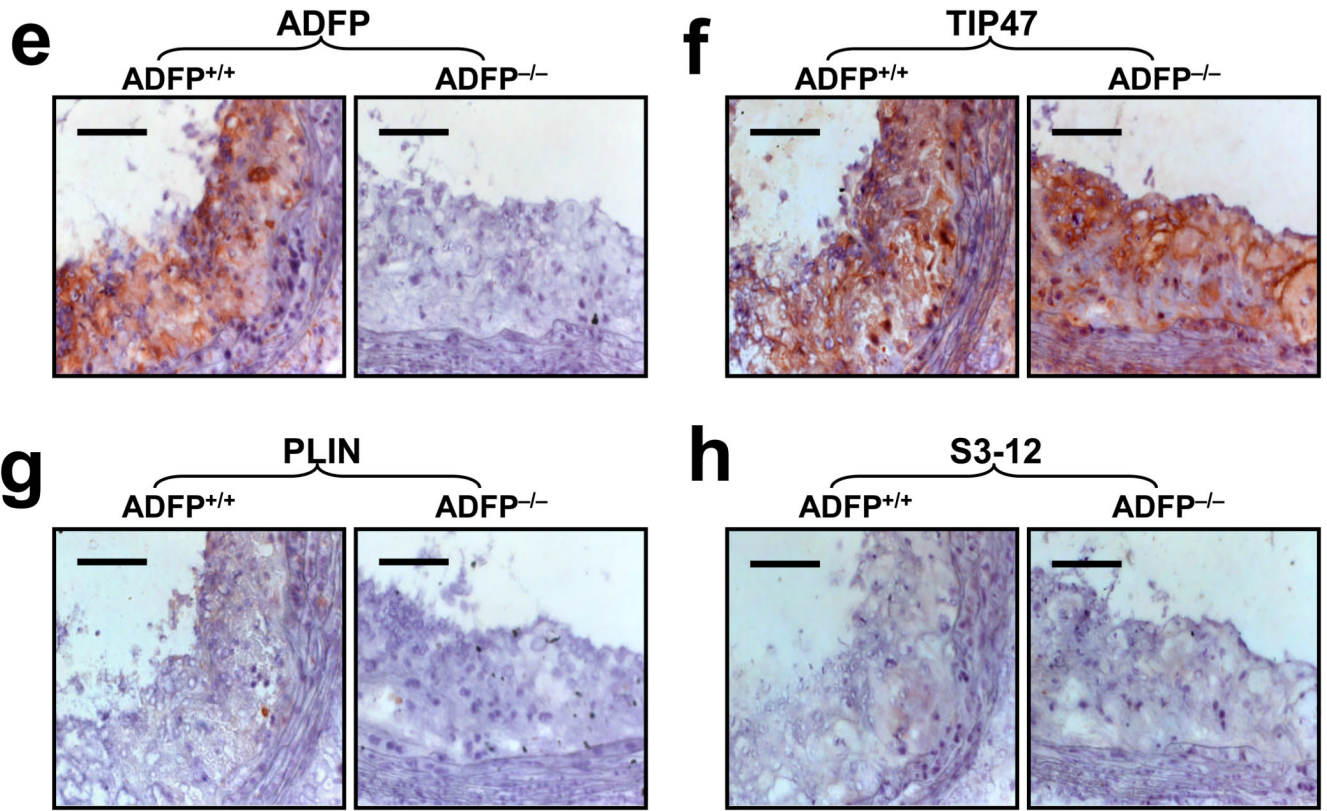
**(a)** Expression of PAT-domain containing proteins mRNA in RAW 264.7 macrophages cultured in the absence or in the presence of acLDL (50 $\mu$ g/ml) (note that ADFP and TIP47 were amplified for 24 cycles, while PLIN and S3-12 were amplified for 35 cycles). **(b)** qPCR analysis of expression of ADFP and TIP47 in RAW 264.7 macrophages that remained untreated or were treated with 50 $\mu$ g/ml of acLDL (n=6, \*p<0.05). **(c)** Representative immunoblot and **(d)** integrated optical density (IOD) relative to  $\beta$ -actin (arbitrary units) of expression of PAT-domain containing proteins in RAW 264.7 macrophages cultured under basal conditions or with 50 $\mu$ g/ml of acLDL (n=3, \*p<0.02). Proteins extracted from fatty liver (FL) and white adipose tissue (WAT) were loaded as positive controls. **(e)** qPCR analysis of expression of PAT-domain containing proteins in atherosclerosis-free aortic sinuses of C57BL/6J mice and highly atherosclerotic aortic sinuses of *ApoE*<sup>-/-</sup> mice (n=6, \*p<0.02).



**e****Figure 2.**

(**a–d**) Computer-assisted morphometric measurement and representative sections of atherosclerotic lesion areas of male (**a and c**) and female (**b and d**) *ApoE*<sup>-/-</sup>/*Adfp*<sup>-/-</sup> and *ApoE*<sup>-/-</sup>/*Adfp*<sup>+/+</sup> mice. (**e**) Computer-assisted morphometric measurement of atherosclerotic lesion areas in mice transplanted with BM from *ApoE*<sup>-/-</sup>/*Adfp*<sup>+/+</sup> mice (ADFP<sup>+/+</sup> BM) or *ApoE*<sup>-/-</sup>/*Adfp*<sup>-/-</sup> mice (ADFP<sup>-/-</sup> BM).







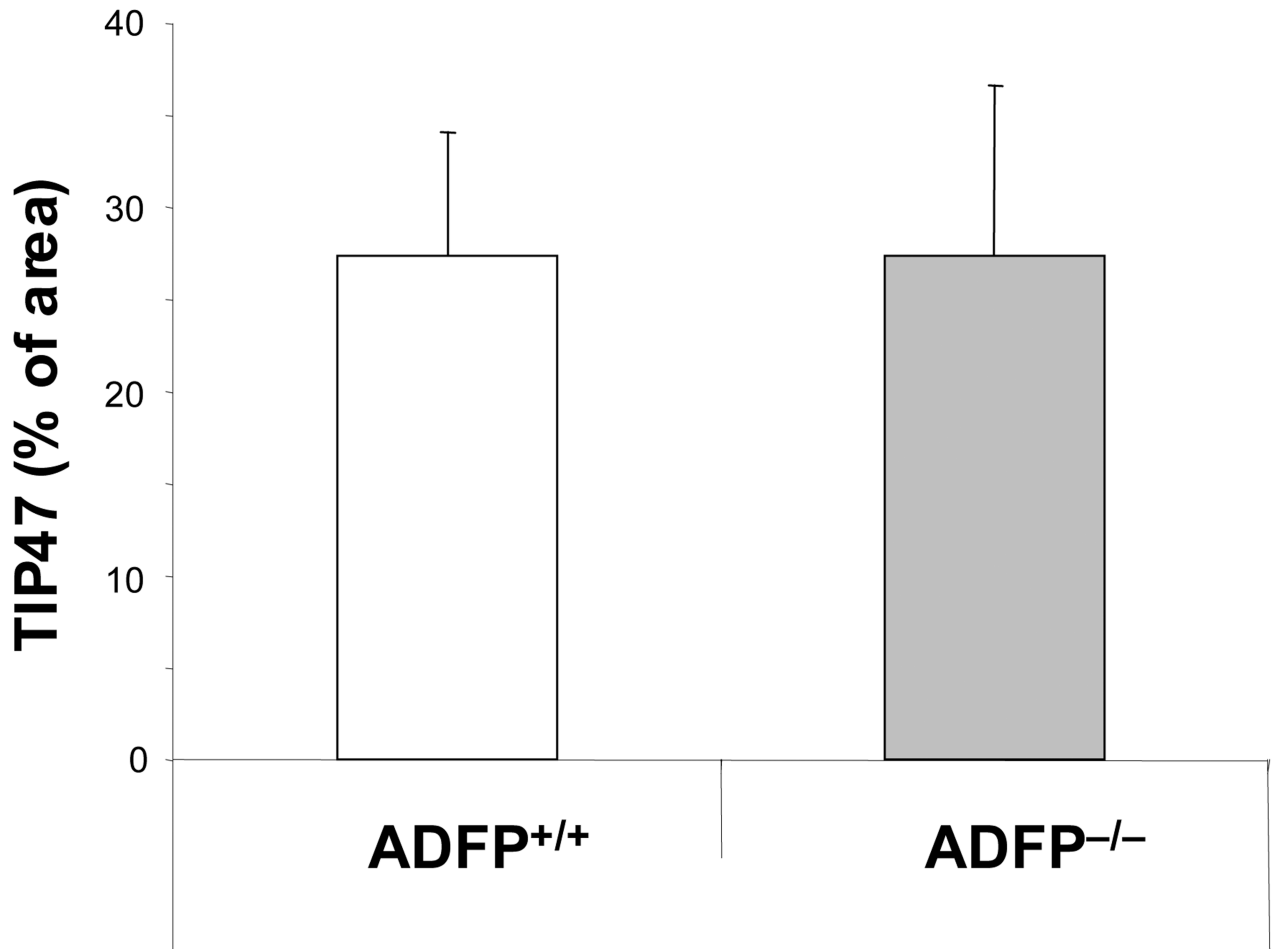


**Figure 3.**

(a) RT-PCR (ADFP and TIP47 23 PCR cycles; S3-12 and PLIN 35 cycles) and (b) qPCR analysis (n= 3, \*p<0.05) of the mRNA expression of the main PAT-family proteins in peritoneal macrophages isolated from *ApoE*<sup>-/-</sup>/*Adfp*<sup>-/-</sup> and *ApoE*<sup>-/-</sup>/*Adfp*<sup>+/+</sup> mice cultured with or without 50 µg/ml of oxLDL (WAT= white adipose tissue). (c) Western blot analysis of peritoneal macrophages cultured with or without 50 µg/ml of oxLDL (FL= fatty liver). (d) qPCR analysis of TIP47 mRNA expression in aortic sinuses of *ApoE*<sup>-/-</sup>/*Adfp*<sup>-/-</sup> and *ApoE*<sup>-/-</sup>/*Adfp*<sup>+/+</sup> mice (n=4). (e) Immunoreactive ADFP (brown color), (f) TIP47 (brown color), (g) PLIN and (h) S3-12, in atherosclerotic lesions of female *ApoE*<sup>-/-</sup>/*Adfp*<sup>+/+</sup> (left panels) and *ApoE*<sup>-/-</sup>/*Adfp*<sup>-/-</sup> (right panels) mice. Scale bar = 50 µm. (i) Quantification of % of area positively stained for TIP47 in lesions of *ApoE*<sup>-/-</sup>/*Adfp*<sup>-/-</sup> and *ApoE*<sup>-/-</sup>/*Adfp*<sup>+/+</sup> mice (n=7).

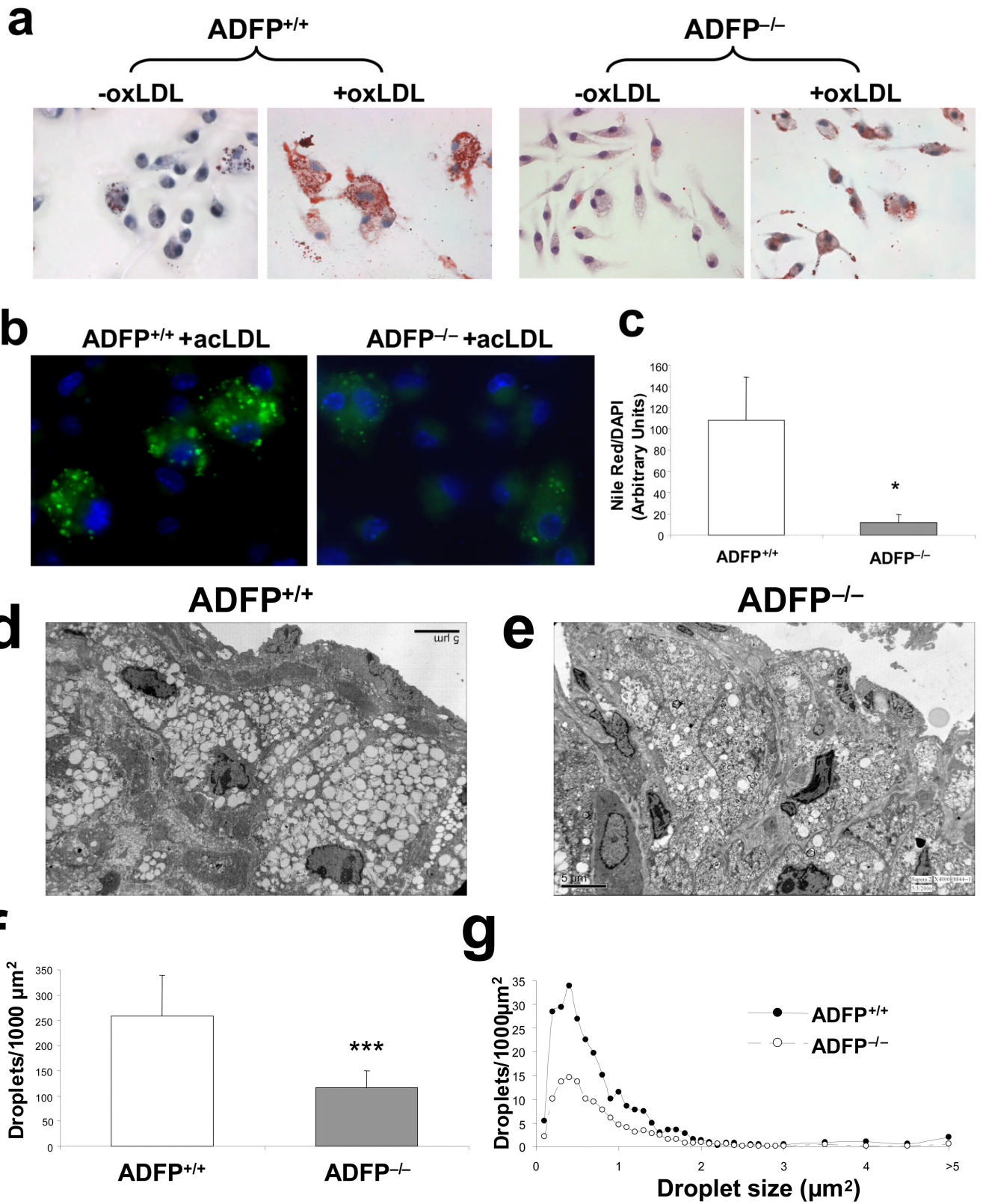
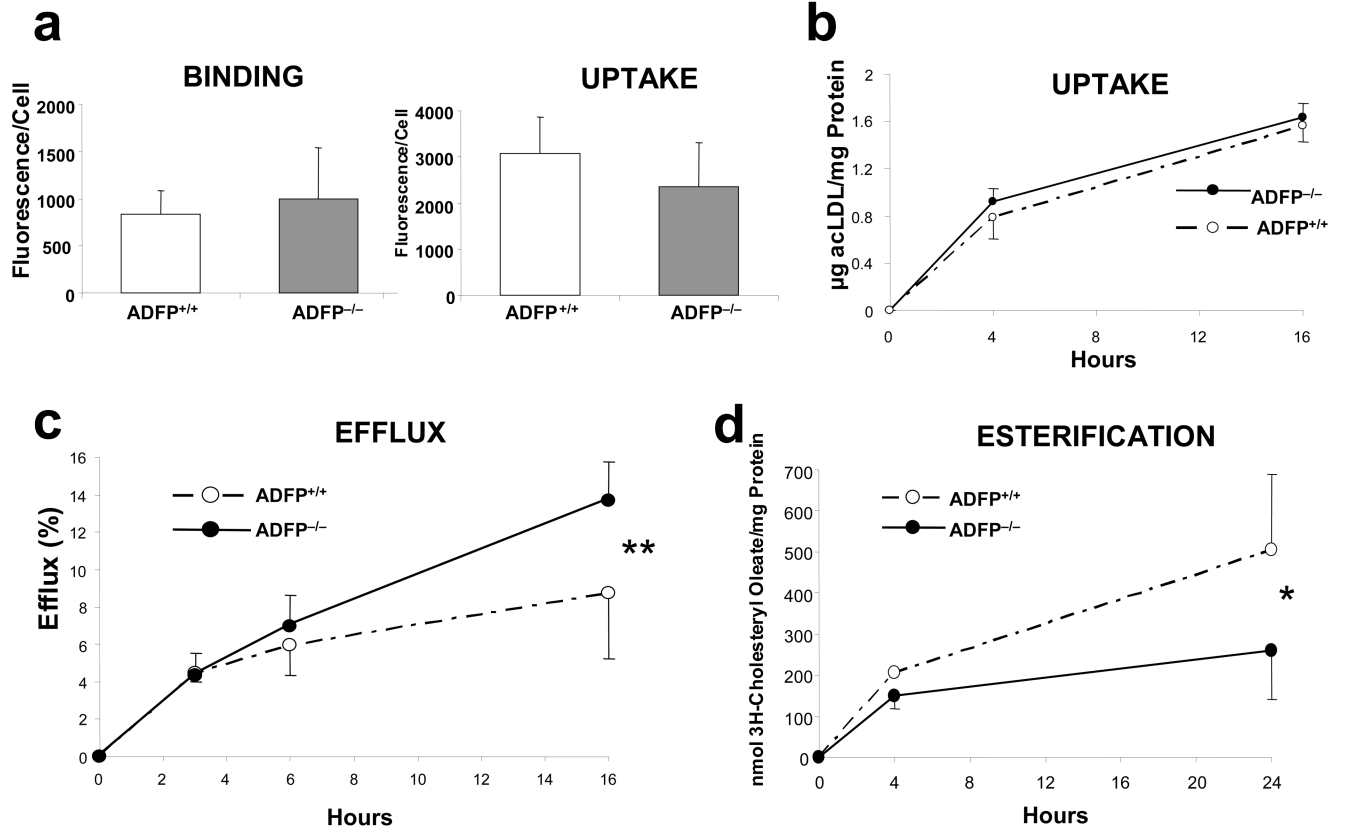
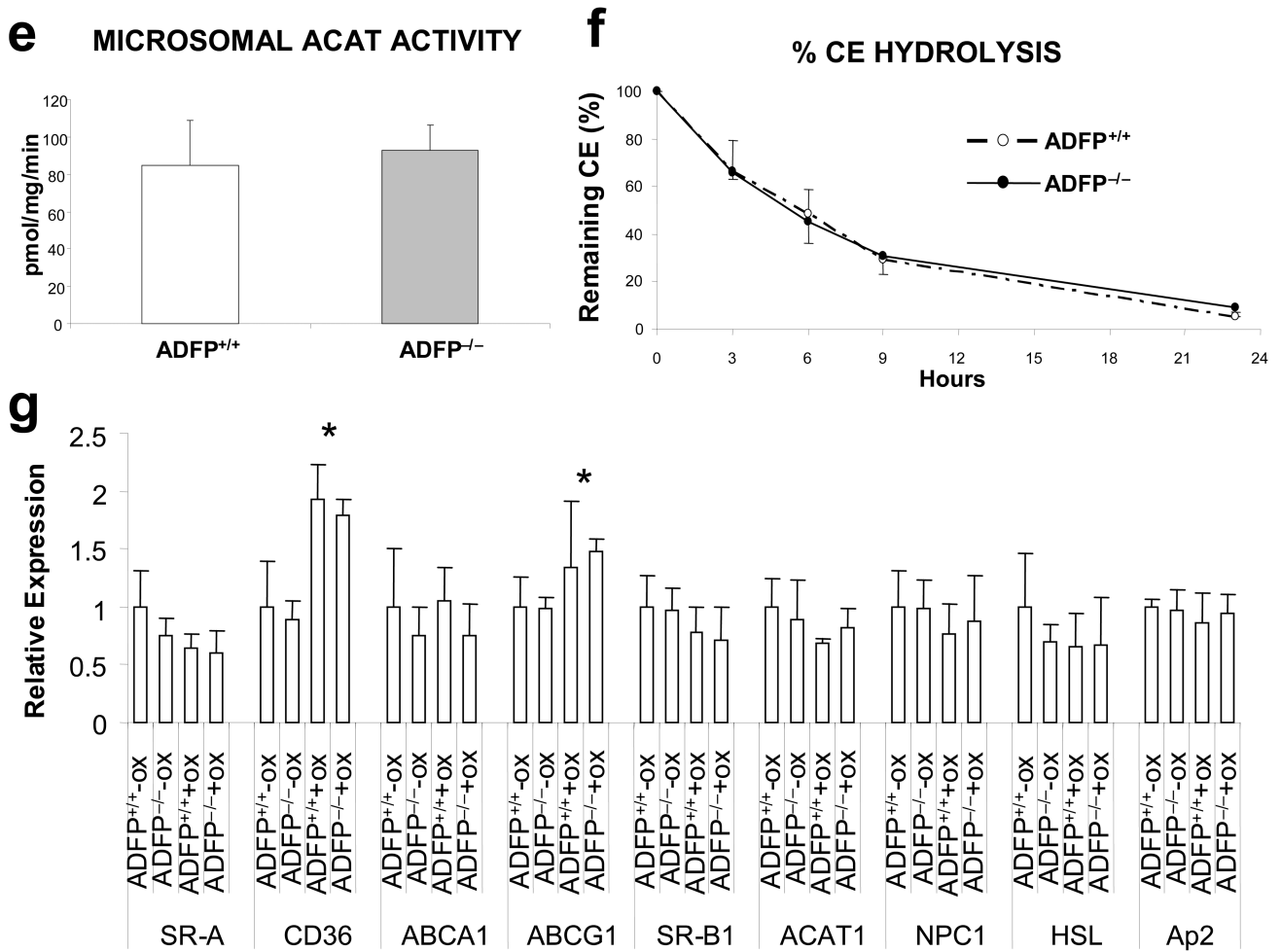


Figure 4.

**(a)** Representative Oil Red O staining of peritoneal macrophages isolated from *ApoE*<sup>-/-</sup>/*Adfp*<sup>-/-</sup> and *ApoE*<sup>-/-</sup>/*Adfp*<sup>+/+</sup> mice that remained untreated (-oxLDL) or were exposed to oxLDL (+oxLDL; 50 µg/ml for 24 h); **(b)** Nile Red staining (green fluorescence) and **(c)** computer assisted quantification of LDs in peritoneal macrophages from *ApoE*<sup>-/-</sup>/*Adfp*<sup>-/-</sup> and *ApoE*<sup>-/-</sup>/*Adfp*<sup>+/+</sup> mice treated with acLDL (50 µg/ml) for 24 h (n=4, \*p<0.02). **(d and e)** Representative EM pictures (4,000×) of atherosclerotic lesions of *ApoE*<sup>-/-</sup>/*Adfp*<sup>+/+</sup> **(d)** and *ApoE*<sup>-/-</sup>/*Adfp*<sup>-/-</sup> **(e)** mice. **(f)** Computer-assisted quantification of the number of LDs per area of lesion (n=9, \*\*\*p<0.001). **(g)** Size distribution of LDs (expressed by area) in foam cells of *ApoE*<sup>-/-</sup>/*Adfp*<sup>-/-</sup> and *ApoE*<sup>-/-</sup>/*Adfp*<sup>+/+</sup> mice.





**Figure 5.**

(a) DiI-acLDL binding (left) and uptake (right) in peritoneal macrophages isolated from *ApoE*<sup>-/-</sup>/*Adfp*<sup>+/+</sup> (n=3) and *ApoE*<sup>-/-</sup>/*Adfp*<sup>-/-</sup> (n=4) mice. (b) Time course of uptake of [<sup>3</sup>H]cholesterol-labelled acLDL in peritoneal macrophages isolated from *ApoE*<sup>-/-</sup>/*Adfp*<sup>-/-</sup> and *ApoE*<sup>-/-</sup>/*Adfp*<sup>+/+</sup> mice (n=4). (c) Time-course of cholesterol efflux to apoA-I in peritoneal macrophages from *ApoE*<sup>-/-</sup>/*Adfp*<sup>-/-</sup> and *ApoE*<sup>-/-</sup>/*Adfp*<sup>+/+</sup> mice (n=9, \*\*p<0.01). The efflux is expressed as % of cholesterol effluxed with respect to the total cholesterol (intracellular + extracellular). (d) Time-course of the rate of intracellular cholesterol esterification (n=5, \*p<0.05). (e) ACAT activity in isolated microsomes (n=4). (f) Time course or CE hydrolysis in [<sup>3</sup>H]cholesterol-labeled macrophages in which CHOL re-esterification was blocked with the ACAT inhibitor CP 113818 (10 μM) (n=4). (g) qPCR of analysis of proteins involved in intracellular lipid homeostasis in macrophages. Note that there were no changes between cells that express or do not express *Adfp* (\*p<0.05 of cells cultured with 50 μg/ml of oxLDL vs. untreated cells; n=3).